Numerical Simulation of the Shaped Charge

Devon Downes[1], Amal Bouamoul[2], Manouchehr Nejad Ensan[1]

[1]NRC Aerospace, National Research Council, Ottawa, ON, Canada
[2]Defence Research & Development Canada–Valcartier, Quebec City, QC, Canada

Devon.Downes@nrc-cnrc.gc.ca, Manouchehr.Nejad@nrc-cnrc.gc.ca, Amal.Bouamoul@drdc-rddc.gc.ca

Abstract: The shaped charge jet formation, fragmentation and penetration in rolled-homogenous armour (RHA) steel target plates were investigated using the explicit, nonlinear lagrangian finite element method. The investigation was conducted in two-dimensions axisymmetric for a shaped charge with a 40mm cone diameters. The results obtained using numerical simulations were compared to the experimental results obtained from experimental tests. In addition, the dynamic behaviour of the jet and target were compared to the visual data obtained from X-rays to confirm jet formation, fragmentation and penetration predictions.

1. Introduction

A shaped charge (SC) is an explosive device with a conical cavity lined with metal, traditionally one with high ductility such as copper. When the detonation wave generated from the explosion reaches the metal liner the intense pressure causes the tip of the cone to collapse forming a high velocity molten jet. The jet can reach velocities of 6-10 km/s and is capable of piercing the strongest of armour due to its concentration of kinetic energy. The objective of any SC is to achieve the longest un-fragmented jet to take advantage of the increased mass associate with the kinetic energy equation.

The first successful application of the SC was made by the British who successfully used the world's first anti-tank rifle grenade, utilizing SC technology. The US produced a High Explosive Anti-Tank (HEAT) machine gun and later the machine grenade was modified to include a rocket motor and a shoulder launcher and became known as the bazooka. The Germans introduced Hohlladung which was used against light ships. The largest of these were the Mistel warheads which were used against ground fortifications [1].

During the 1960s and 1970s, SC theory developed further improvements to explosives over TNT to more energetic compositions such as Composition B [2] and improvements to initiation techniques such as wave shaping techniques [6]. The largest single advance to SCs stemmed from the development of hydrocodes such as SHELL [3] which helped to facilitate a better understanding of liner collapse, jet fragmentation and jet penetration. Numerical codes used continuum mechanics of the mass, momentum and energy equations, together with appropriate material models to simulate and predict SC performance. Holmquist *et al* [4] used experimental data of cylinders impact tests to develop constants for material models. Specifically of importance was the Johnson-Cook material model, which is used when high strain rates are present such as those present in liner deformation. With the appropriate material model the main focus of liner collapse theory consisted of obtaining the longest, non-fragmented, high density jets in order to achieve a high kinetic energy on impact. Because of its high ductility, copper was generally regarded as the material of choice for liners, although molybdenum [5], tantalum [6], tungsten [7] and alloys of copper-tungsten [8] were researched as a means of increasing the material density and its effectiveness against modern armor.

Although different numerical approaches for analysis of the SC impact events are available, finite element analyses, which are based on accurate constitutive models, provide the most detailed information on the spatial and temporal distribution of impact events. The objective of the present research was to simulate the transient dynamic impact resulting from a collision between a SC and target plates, using LS-DYNA [9] finite element analysis software. LS-DYNA is an explicit, nonlinear finite element code used for SC impact analysis. It is also widely used by the defence and military to simulate structural failure, air/ water/ soil and container explosion. Features of this code include large material and element libraries, many contact algorithms and a high level of accuracy.

This paper presents a Langrangian approach to simulate liner collapse, fragmentation and penetration to RHA steel. LS-DYNA, an explicit, nonlinear finite element analysis program was used in the simulation efforts. The

results obtained using this simulation were compared to the experimental results to verify the validity and accuracy of the model.

2. Numerical Simulation

Analytical models, although limited in scope, are quite useful for developing an appreciation for the dominant physical phenomena occurring in a given SC impact. If a complete solution to SC jet formation and fragmentation is necessary, recourse must be made to numerical simulation. This is especially true for oblique impacts or situations where a three dimensional stress state is dominate, for which there are virtually no analytical models that can deal with such complexity.

Although different numerical approaches for analysis of the SC impact events are available, finite element analyses, which are based on accurate constitutive models, provide the most detailed information on the spatial and temporal distribution of impact events. The objective of the present research was to simulate the transient dynamic impact resulting from a collision between a SC and target plates, using LS-DYNA finite element analysis software. LS-DYNA is an explicit, nonlinear finite element code used for SC impact analysis. It is also widely used by the defence and military to simulate structural failure, air/ water/ soil and container explosion. Features of this code include large material and element libraries, many contact algorithms and a high level of accuracy.

Full scale simulation of the SC meant three-dimensional (3D) analysis using solid elements. While this type of simulation is possible in LS-DYNA it is computationally taxing in terms of time and yield results which are not necessarily more accurate than its two-dimensional (2D) counterpart. As a means of model simplification while still capturing the essentials of the SC, in this work, the SC was modeled as a 2D axisymmetic (along the y-axis).

2.1 Finite Element (FE) Model

The two-dimensional axisymmetric model developed to study the SC impact is shown in Figure 1. The axisymmetric nature of the simulation provided a reduction (over full scale simulation) by reducing the number of elements thereby reducing the computation time without sacrificing accuracy of the results. This model was divided into five major parts: the detonator, the explosive, the liner, the top casing and the side casing. Consistent with the experimental tests, a 40mm SC cone diameter was used. The SC had an apex angle of 53° and used approximately 2400 shell elements to model the five major components.

Three targets were made of RHA-Steel. The targets were modelled as infinite targets in the length direction and carried a thickness of 0.6cm. They were placed at a standoff distance of seven (7) times the cone diameter of the SC, which is the maximum standoff distance for performance as discussed in [2, 10]. Only half of the target was modeled with the other half being accounted for by the axisymmetric design of the simulation as shown Figure 1. The targets were modeled using approximately 2500 shell elements for each target.

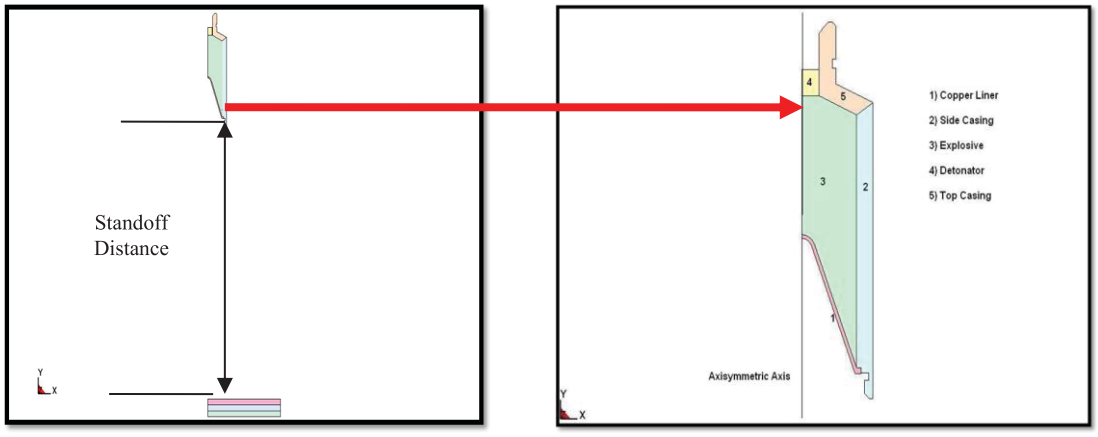

Figure 1: Developed Finite Element Model of the SC.

2.2 Material Constitutive Model

LS-DYNA currently contains more than two hundred and thirty nine constitutive models to cover a wide range of material behaviour. The material definition used in simulation efforts are described as: 1) High explosive Burn 2) Jones-Wilkins-Lee 3) Elastic Plastic Hydrodynamic 4) Mei-Gruneisen.

2.2.1 Explosive and Detonator

The detonator and explosive provided the planar pressure wave needed to deform the liner into the jet. Both parts were modeled using the High Explosive Burn material model and the Jones-Wilkins-Lee equation of state (JWL-EOS). This particular burn model controls the releases of chemical energy while the JWL-EOS controls the pressure wave associated with the release of the chemical energy.

2.2.1.1 High Explosive Burn

The explosive was simulated using the High Explosive Burn model along with the Jones-Wilkins-Lee equations of state (JWL - EOS) which controls the release of chemical energy. High Explosive Burn controls the pressure in an element associated by equation 1, the pressure from the equation of state, p_{eos}, the relative volume, V, and the internal energy density per unit volume are multiplied by a burn fraction F.

$$p = Fp_{EoS}(V, E) \qquad (1)$$

Burn fractions are dimensionless parameters calculated to spread the burn front over several zones and is given by equation 2. The spread ensures the detonation of the explosive is applied smoothly across the mesh.

$$F_1 = \frac{2(t-t_1)DA}{3v_e} \quad (2)$$

Where t is the current time and t_1 represents the lighting time, defined as the distance from the detonation point to the center of each zone divided by the detonation velocity (D). A is the area density and ν is the specific volume.

2.2.1.2 Jones-Wilkins-Lee Equation of State

The High Explosive Burn material model requires an equation of state (EOS). EOS is required to accurately simulate material behaviour when shock waves are present in the simulation. The JWL-EOS is a mathematical expression which characterizes the chemical reactions in predefined zones in an explosive mesh. It uses energy and volume relationships associated with chemical detonations products to calculate the pressure using equation 3 [11].

$$p = A\left(1 - \frac{\omega}{R_1 V}\right)e^{-R_1 V} + B\left(1 - \frac{\omega}{R_2 V}\right)e^{-R_2 V} + \frac{\omega E}{V} \qquad (3)$$

The pressure is related to the relative specific volume V_0, where V is defined by the specific volume (v) at the interested time divided by the initial specific volume v_o. E contains the chemical bond energy as well as kinetic energy associated with the momentum aspect of flow. A and B are pressure coefficients associated with the particular explosive used. R_1 and R_2 are the principal and secondary eigenvalues. ω is the fractional part of the normal Tait equation adiabatic exponent [12].

2.2.1.3 Copper Liner

The liner was made of oxygen-free high thermal conductivity copper (OFHC-Copper) in the experimental testing. This type of copper is taken as 99.99% pure copper with only 0.0005% oxygen content. Some studies have shown that impurities in the liner can lead to brittle breakup and perturbations in the initial jet formation

process [13]. Using OFHC copper mitigates any influence other materials may have on the jet formation behaviour. The OFHC copper was modeled using the Elastic Plastic Hydrodynamic material model. In addition, since the copper experienced high strain rates, the Gruneisen – EOS was used.

2.2.1.4 Mei-Gruneisen-EOS

The Mie-Gruneisen EOS relates pressure as a function of density and internal energy in solid materials using equation 4 when the solid is in expansion

$$P = \frac{\rho C^2 \mu \left[1+\left(1-\frac{\gamma}{2}\right)\mu-\frac{a}{2}\mu^2\right]}{\left[1-(S_1-1)\mu-S_2\frac{\mu^2}{\mu+1}-S_3\frac{\mu^3}{\mu+1}\right]^2} + (\gamma + a\mu)E \qquad (4)$$

E is the internal energy of the copper liner, C is the bulk speed of sound in copper, α is a first order correction to γ and γ is the Gruneisen Gamma and is approximated as $\gamma = \frac{\rho_o \gamma_o}{\rho}$, where ρ_o and γ_o are the density and Gruneisen parameter at the reference state of zero-Kelvin and ρ is the density of copper at the interested time. S_1, S_2, S_3 and A are the coefficients defining the slope of the Hugoniot curve for copper and $u = \frac{\rho}{\rho_o} - 1$.

2.2.1.5 Target

The target structure, which is made from Rolled Homogenous Armour (RHA) steel, is uniform throughout its section. The face of the steel is hardened by heat-treatment of rolling and forging during the manufacturing process. This removes any imperfections which could reduce the strength of the steel. Rolling also elongates the grain structure in the steel to form long lines, which enables the stress under which the steel is placed to flow throughout the metal and not be concentrated in one area. The result is an enhanced ballistic performance of the steel attributed to higher level of hardness and ductility (RHA steel does not experience brittle fracture mechanism), because of the above mentioned qualities. RHA steel is largely used in the military application to manufacture armoured vehicles.

3. Results

Numerical simulations using the developed SC finite element models were performed. The impact events were analyzed for a time period of 300μs, which was chosen to be sufficiently long to simulate the initial events of the impact. Dynamic results were recorded at 0.5μs equal time steps.

Three primary validation criteria were used to ensure a useful simulation of the model. These were jet formation, jet fragmentation and jet penetration into the target plates. If the simulation results compared favourably with experimental test results in those three categories, then it was concluded that the models were representing the test results accurately and subsequent simulations could be used to analyze the SC and the armour and anti-armour systems.

3.1 Jet Formation

After initiation of the detonator a shock wave propagates through the explosive carrying shock strength of approximately 16GPa after 3μs after initiation and growing to 22GPa 5μs after initiation as shown in Figure 2a and Figure 2b, respectively for the 40mm SC. The location of shock wave can be observed very clearly by the expansion of the explosive and mesh deformation as shown in these figures. When the shock wave contacts the liner, its strength has grown to 30GPa and an intensive remeshing of the copper liner begins due to the liner deformation under the tremendous amount of pressure. The apex of the liner is accelerated to its final velocity of 6685m/s while the slug trails behind at 450m/s and maintains this velocity until impact. This is in line with the experimental results which show the jet tip velocity at 7276 m/s, an 8% difference between experimental and

simulation results. The difference between the jet tip velocity and slug also means the liner experiences a strain rate of approximately 32,000s^{-1} and is consistent with the magnitude of strain rates experience by liners reported in [7].

Qualitative comparison of FE simulation with X-ray image from the experimental test for this case is also presented in Figure 4. It can be seen from these figures that the FE model correlated very well with the experimental results for the jet formation.

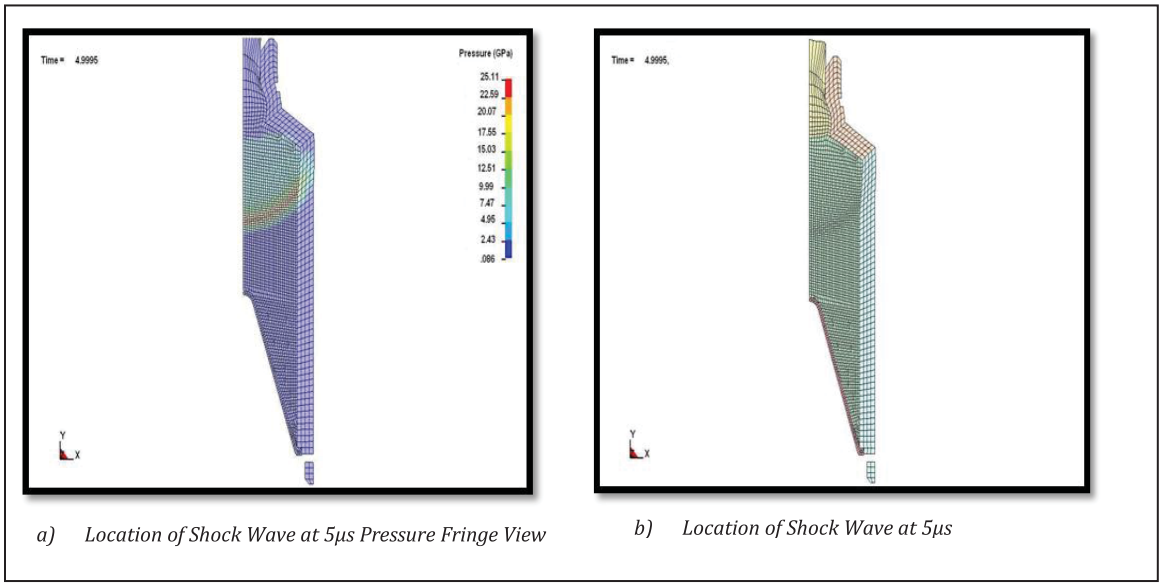

a) Location of Shock Wave at 5μs Pressure Fringe View

b) Location of Shock Wave at 5μs

Figure 2: Shock Wave Propagation.

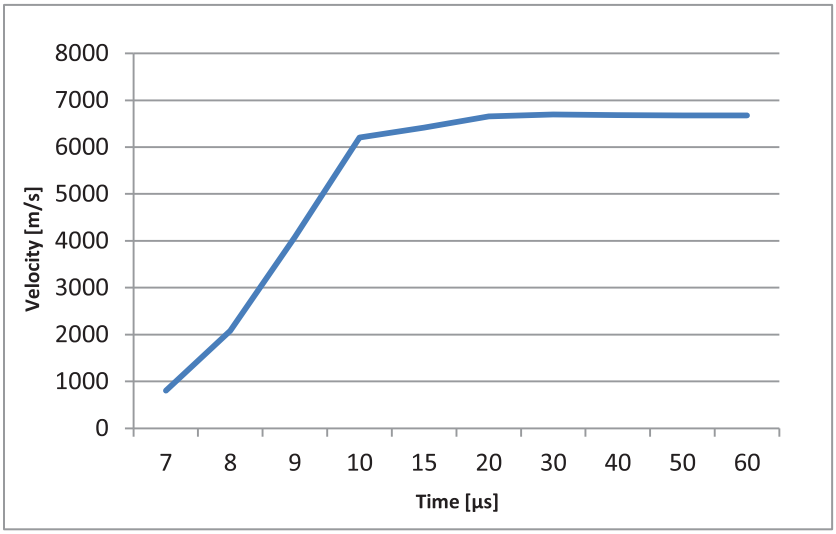

Figure 3: Velocity versus Time Graph 40mm SC Jet Tip.

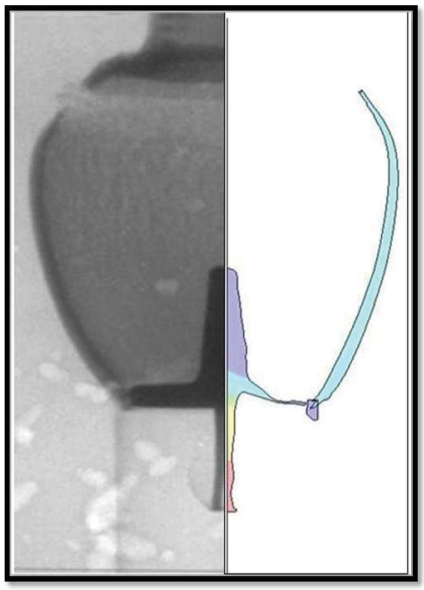

Figure 4: Comparison of FE Simulation with X-ray Image (X-ray Image provided DRDC-V).

3.2 Jet Fragmentation

The comparison of jet fragmentation obtained from FE simulation and X-ray photography is presented in Figure 5. After 41µs the jet starts to fragment, with the first fragmentation occurring at approximately 1/3 (70mm) of the jet length on the tip side of the 40mm SC. This is consistent with experimental results.

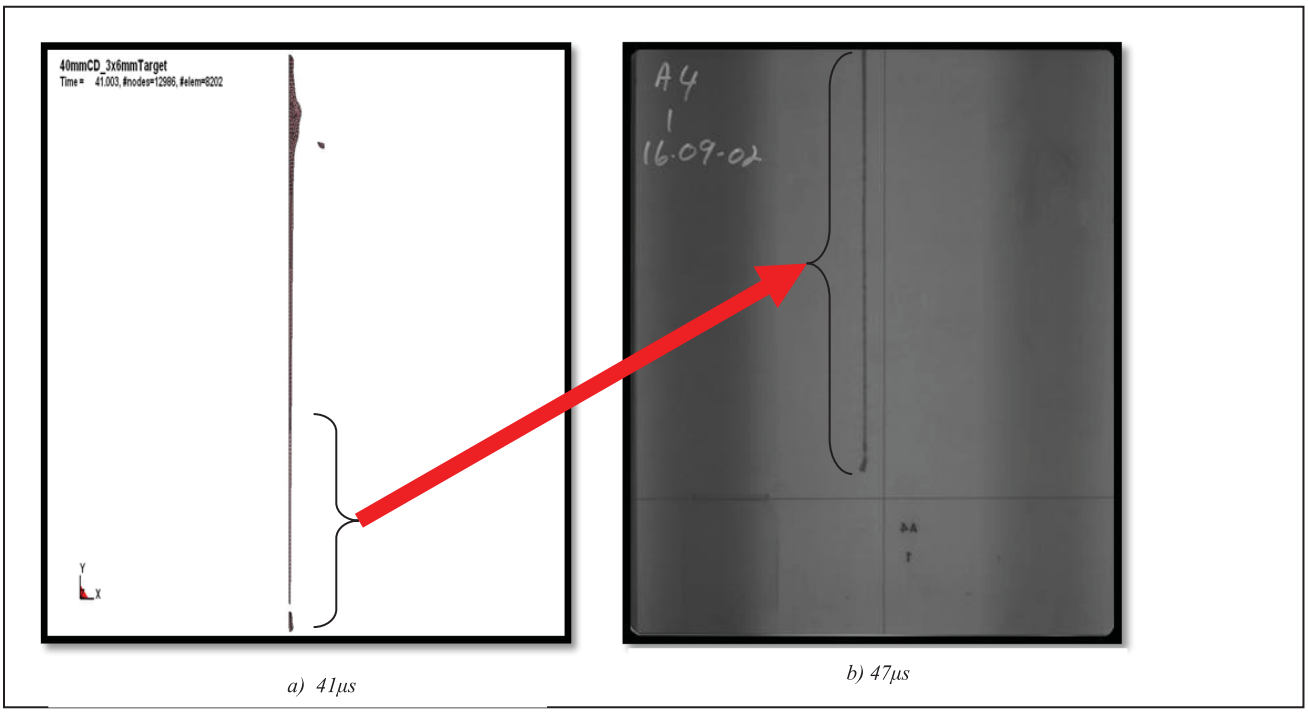

a) 41µs *b) 47µs*

Figure 5: Jet Fragmentation of the 40mm SC.

3.3 Target Impact: Penetration

The standoff distance was chosen to be seven times the cone diameter of the SC as recommended by the DRDC-V. At this standoff distance the maximum penetration is expected as reported by [2, 10]. In each of the setup configurations the targets were too thin to prevent complete penetration of the SC. To resist penetration, target thickness is estimated to be approximately six times the SC diameter as reported in [2]. In the case of the 40mm SC, impact occurred at 60μs after initiation of the detonator, with the first fragment of the SC impacting the target with a velocity of 6686m/s while the simulated impact velocity was 7276m/s. This represented an 8% difference between experiment and simulated results.

Upon impact the target elements erode away forming a crater of 12mm diameter in the front of the target and a lesser diameter hole of 6mm in the rear of the target. The front hole diameters obtained from simulation are in good agreement with experimental data being within 10% deviation.

4. Conclusion

A new finite element model has been developed for a shaped charge based on the Lagrangian formulation. This model has been successfully demonstrated in the simulations of shaped charge penetration into target plates. The finite element model of the shaped charge provided data on the jet formation, fragmentation and penetration into target plates that compared very well to experimental data. There was good correlation between test results and numerical simulation, this correlation provides confidence in the use of this approach to model shaped charges for other designs. For instance, the geometry of the shaped charge could be optimized in terms of different cone material, angle and shape to improve the shaped charge's performance of the shape charge. In addition, the numerical simulation presented in this report may be used as an effective tool to reduce the number of experimental tests required to develop new methods of mitigating the effects of SC on armoured vehicles.

Acknowledgements

The authors would like to thank Defence R&D Canada_Valcartier (DRDC_V) and the National Research Council of Canada (NRC) for sponsoring this collaborative project.

References

[1] Walers, W., "*A brief history of Shape Charg*es", 24th International Symposium on Ballistics, New Orleans, Vol.1, September 22-26, pp. 3-10, 2008.

[2] Walters, and Zukas, J. A., "*Fundamentals of Shape Charges",* John Wiley & Sons, New York, 1989.

[3] Johnson, W.E., *"A Two-Material Version of TRIOIL Code with Strength",* Computer Code Consultants, Los Alamos, New Mexico, 1976.

[4] Johnson G.R., and Holmquist, T.J., "*Evaluation of Cylinder-impact test data for constitutive model constants*", Journal of Applied Physics, Vol. 64, Issue 8, pp. 3901-3910, May 1988.

[5] Cowan K.G., and Bourne B., "*Analytical Code and Hydrocode Modelling and Experimental Characterisation of Shaped Charges Containing Conical Molybdenum Liners*", 19th International Symposium on Ballistics, Interlaken Switzerland, May 7 - 11, 2001.

[6] Murr L.E, Shih H.K., Niou C-S., "*Dynamic Recrystallization in Detonating Tantalum Shaped Charges: A Mechanism for Extreme Plastic Deformation*" Materials Characterizations, Vol. 33, Issue 1, pp. 65-74, July 1994.

[7] Lee S., Hong M-H., Noh J-W., and Baek W. H., "*Microstructural Evolution of a Structural Shape Charge Liner and Target Material During Ballistic Tests*", A Metallurgical and material Transaction, vol. 33, No. 4, pp. 1069-1074, April 1st 2002.

[8] Lassila, D.H., *"Mechanical Behaviour of Tungsten Shape Charge Liner Material"* 14th International Symposium on Ballistics, Quebec City, September 26-29, August 1st 1993.

[9] Hallquist, J.O., "*LS-DYNA Keyword User's Manual*", Version 971, Livermore Software Technology Corporation, Livermore, CA, 2007.

[10] Molinari, J.F. *"Finite Element Simulation of Shaped Charges",* 13th Meshing Round Table Proceedings, Williamsburg, Virgina, pp. 81-94, September 19-22, 2004.

[11] Urtiew, P.A., and Hayes, R. *"Parametric Study of the Dynamic JWL – EoS of the Detonation Products"*, Combustion, Explosion and Shockwaves, Vol. 27, No. 4. pp. 126 - 137, July – August, 1991.

[12] Neece, A.G., and Squire, D.R., *"On the Tait and Related Empirical Equations of State"*, The Journal of Physical Chemistry, Vol. 72, No.1, pp. 128-136, January 1968.

[13] Ayisit, O., *"The influence of Asymmetries in Shape Charge performance"*, International Journal of Impact Engineering, Vol 35, Issue 12, pp. 1399-1404, December 2008.

[14] Johnson, G.R. and Cook, W.H., *"A Constitutive and Data for Metal Subjected to Large Strains, High Strain Rates and High Temperatures"* 7th International Symposium on Ballistics, Hague, Netherlands, pp. 541 – 547, 1983.

[15] Radovitzky, R., and Ortiz, M., *"Error Estimation and Adaptive Meshing in Strongly Nonlinear Dynamics Problems"* Computer Methods Applied Mechanics Engineering, Volume 172, pp. 203 – 240, 1999.